Geofísica Internacional (2005), Vol. 44, Num. 3, pp. 251-263

Geoelectrical characterization of an oil-contaminated site in Tabasco, Mexico

Vladimir Shevnin[1], Omar Delgado-Rodríguez[1], Luis Fernández-Linares[1], Héctor Zegarra Martínez[1], Aleksandr Mousatov[1] and Albert Ryjov[2]

[1] *Mexican Petroleum Institute, Mexico, D. F., Mexico*

[2] *Moscow State Geological Prospecting Academy, Geophysical Faculty, Moscow, Russia*

Received: September 21, 2004; accepted: January 27, 2005

RESUMEN

La caracterización geoeléctrica de un sitio contaminado por hidrocarburos, donde hace treinta años fue perforado un pozo petrolero, fue realizada utilizando el método de Sondeo Eléctrico Vertical (SEV) con la tecnología de Imagen de Resistividad e Interpretación 2D de los datos adquiridos. La interpretación de los datos de SEV estuvo apoyada por mediciones de resistividad en muestras de agua y suelo. Las zonas contaminadas corresponden con anomalías de baja resistividad ubicadas encima del nivel freático. Los resultados de la interpretación geoeléctrica fueron comparados con los resultados del muestreo geoquímico. La correlación inversa existente entre la resistividad eléctrica y la concentración de contaminantes confirma la existencia de contaminación madura, la misma que crea anomalías de baja resistividad. Mediante la modelación petrofísica es posible estimar el valor de resistividad que define la frontera entre zona limpia y contaminada. Los datos de resistividad son presentados a manera de secciones y mapas, además de haber sidos recalculados a secciones y mapas de parámetros petrofísicos, como herramientas útiles en la caracterización más precisa y detallada de las zonas contaminadas.

PALABRAS CLAVE: Sondeo Eléctrico Vertical, 2D tecnología de resistividad, contaminación por hidrocarburos, modelación petrofísica.

ABSTRACT

A geoelectrical characterization of an oil-contaminated site, where thirty years ago an oil well was drilled, was carried out using vertical electrical sounding (VES) method on 2D Resistivity Imaging technology and 2D interpretation. VES data were added by water resistivity measurements and soil resistivity analysis. The contaminated zones feature with low resistivity anomalies situated above groundwater level. The geoelectrical interpretation was compared with geochemical sampling. An inverse correlation between electrical resistivity and concentration of contaminants confirms that the oil-contamination is mature and for this reason it creates low resistivity anomalies. Petrophysical modelling allowed estimating boundary resistivity value separating clean and contaminated zones. Resistivity data were visualized as cross-sections and maps and also were recalculated into sections and maps of petrophysical parameters, useful for more precise and detailed characterization of contaminated zones.

KEY WORDS: Vertical Electrical Sounding, 2D Resistivity Imaging, oil contamination, petrophysical modelling.

INTRODUCTION

The exploration and activity of production in the oil industry generates a large volume of wastes. It was estimated that 73% (125 867 tons) of hazardous wastes from oil processing by the Mexican oil industry per year 2000 consisted of drilling mud and cuttings (PEMEX, 2001). Unlike the US Petroleum Exemption (USEPA, 2002), Mexican environmental regulations establish that drilling mud and cuttings are hazardous wastes. Therefore intensive research and adaptation of technologies and methods are required to localize contaminated zones and to control remediation processes in the subsurface.

Geophysical methods are frequently employed in the characterization of a contaminated site. Previous investigations have demonstrated the efficiency of geoelectrical methods in the delineation of contaminated zones, both in area and with depth (Abdel-Aal *et al*., 2001, Sauck, 1998); Vertical Electrical Sounding (VES) on Resistivity Imaging technology has proven to be an effective technique (Modin *et al*., 1997; Shevnin *et al*., 2002; Shevnin *et al*., 2003).

Oil contamination of soil, after four months to one year after contamination, creates a low resistivity zone (Sauck, 1998; 2000). The chemical processes in oil-contamination have been described in detail by Bailey *et al*. (1973), Sauck (1998, 2000) and Atekwana *et al*. (2001) in terms of reactions and variations in the physical characteristics of the affected media. According to these authors, low resistivity anomalies result from an increase in the level of Total Dissolved Solids (TDS) created by bacterial action in the deeper part of the vadose zone or below the water table, in an acid environment.

We present the results of VES application to the characterization of a polluted site in Mexico. The geoelectrical results are correlated with geochemical information. We used Resistivity Imaging technology (Griffiths and Barker, 1993), 2D VES data interpretation (Loke and Barker, 1995), soil resistivity tests in the laboratory and recalculation of resistivity data into petrophysical parameters, in order to obtain a better characterization of oil contamination.

GENERAL SITUATION

The study area is an abandoned oil well situated near Cardenas, Tabasco, Mexico, and measures 160 m x 180 m (Figure 1). The well was abandoned 13 years ago after 20 years of production. In the early 1970s, drilling mud and oil-soaked rock cuttings were disposed in a pit in the lower part of the area. For most of the year it is filled in with water (Figure 1). The study area can be divided into two zones: the swampy pit zone and the dry elevated zone.

FIELD INVESTIGATIONS

Vertical Electrical Sounding (VES)

A total of 246 VES points, distributed along 11 profiles, were measured in the study area (Figure 1) to determine the geoelectrical structure in the upper 10 metres, to delineate the oil contaminated zones both in plan and in depth, and to estimate the level of contamination.

A VES survey was carried out using a great number of electrodes (~50) placed along each profile with a constant interval (2 m). AB/2 spacing of a Schlumberger array was from 2 to 20 m with the step 2 m. Spacing between sounding centres was 4 m.

We used ERA resistivity meter developed in Russia, operating at a frequency of 4.88 Hz with a sensitivity of 1 μV, with a stabilized current of 10 mA.

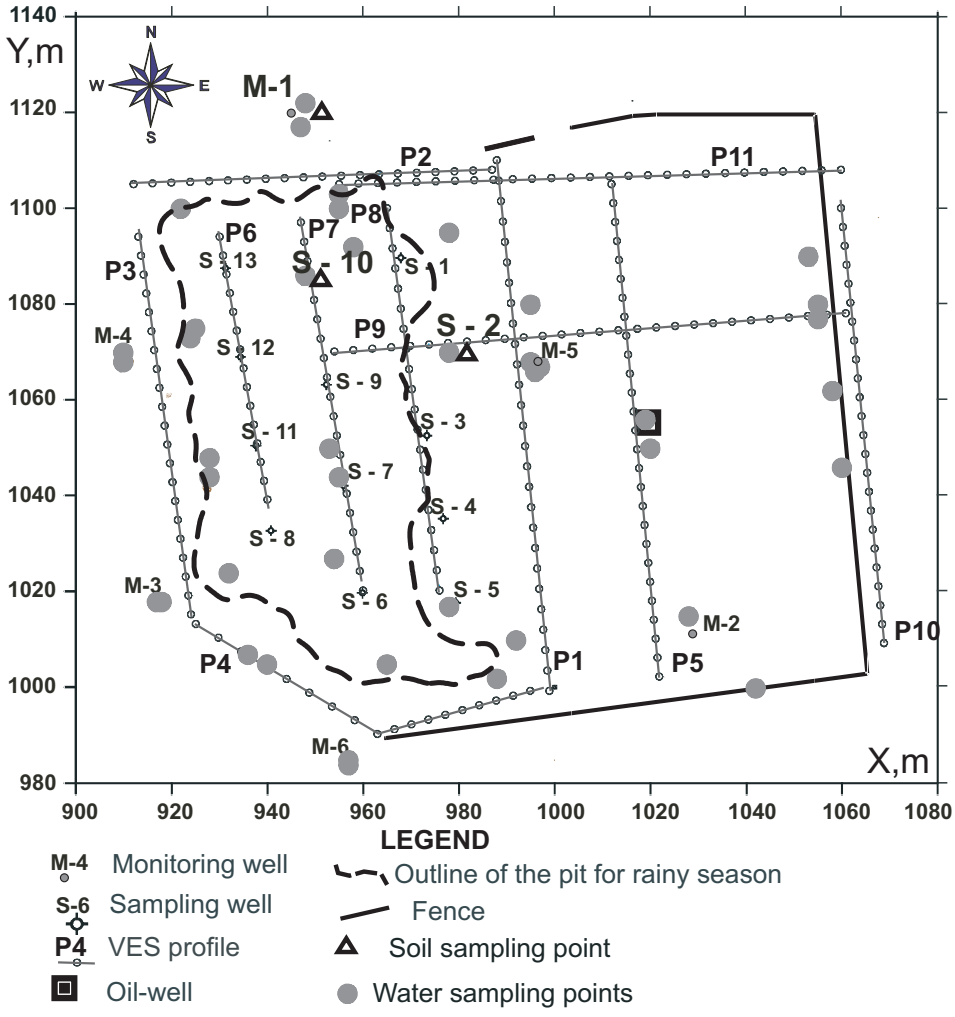

Fig. 1. Map of the study area.

Water resistivity measurement

Water resistivity was measured in 44 water samples (Figure 1) in the study area. This survey included water from the regional aquifer and surface water (mainly from the pit). Six wells (M-1 to M-6) were drilled to 4 m depth to monitor ground water around the site. The surface water included uncontaminated and contaminated samples. The measurements were carried out using the resistivity equipment and a calibrated four-electrode cell (resistivimeter) designed for water resistivity measurements.

Soil resistivity measurement

We performed one reference soil sampling at location M-1 (Figure 1) for geoelectrical purposes. This location is uncontaminated and has high clay content. The soil sample was divided in four equal parts and measured with four resistivimeters. The soil was saturated with water of different salinity (0.23 – 17 g/l NaCl). We obtained ρ(C) dependence to estimate clay content and some others parameters (Figure 7, Table 2). Two additional soil samples were obtained from the contaminated zone near boreholes S-2 and S-10 (Figure 1). These water and soil resistivity measurements established the eventual range of anomalous values resulting from pollution.

Geochemical studies

Soil samples were collected for geochemical analysis from three different depth levels between 0 - 2 m. Thirteen samples (S-l to S-13) were collected inside the pit and two were control samples collected from outside.

The soil samples were collected with a split spoon sampler using percussion. They were immediately stored in clean 250 ml bottles with a Teflon-lined lid, and were preserved at 4°C for analysis, after USEPA (1995) guidelines. Total Petroleum Hydrocarbon (TPH) concentration was determined using infrared spectroscopy after EPA418.1 (USEPA, 1983). Clay content and soil particle size distribution were determined after Bouyoucos (1962).

Values of TPH concentration, clay content and soil electrical conductivity were used to control the geoelectrical anomalies and to correlate the geochemical and geoelectrical data. Geochemical studies were performed mostly inside the pit whereas geoelectrical measurements covered a wider area.

RESULTS AND DISCUSSION

It is not easy to recognise the effect of contaminants on resistivity when clay is present. However, the application of VES Resistivity Imaging technology, supported by measurements of water and soil resistivity and petrophysical modelling, allows discrimination between the contaminated and uncontaminated areas.

Water resistivity

The histogram in Figure 2A was obtained from 44 water samples. It shows the presence of several groups of samples, with mean resistivity values of 11, 15, 23, 46 and 72 Ωm. After comparing water resistivity with location of sampling and geological information, we concluded that the value 46 Ωm corresponded to surface water, the value 23 Ωm to groundwater from the main aquifer (samples from monitoring wells) and the water of 11 and 15 Ωm to polluted surface water. The water of 72 Ωm was found in the concrete basin near the oil borehole. The map of Figure 2B shows the distribution of water resistivity in the area. The lowest values were found in the northern part of the pit and in the monitoring well M-5. A contamination map for the pit area (Figure 2C) shows maximal contamination in the northern (more than 8000 ppm) and southern (more than 2000 ppm) parts of the pit.

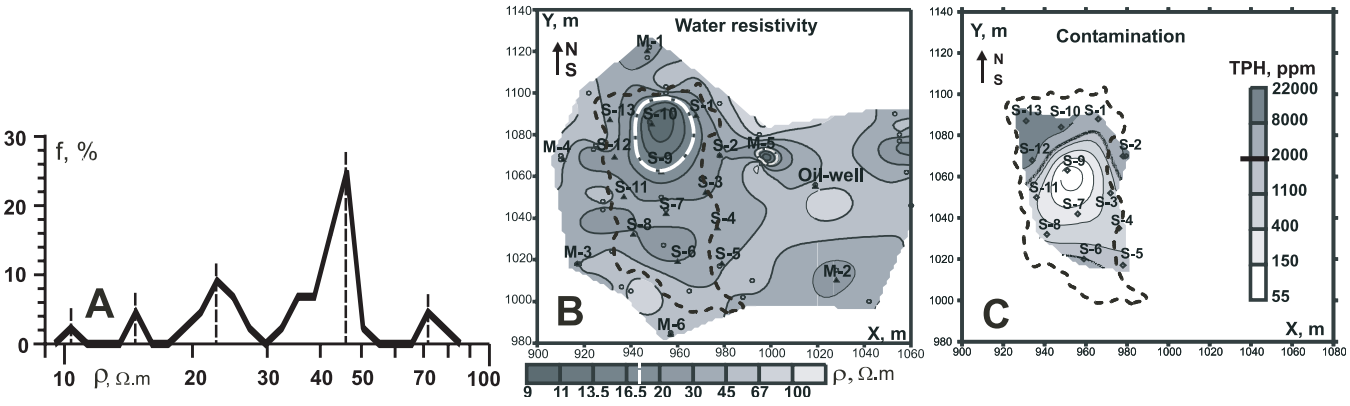

Fig. 2. Histogram (A) and map (B) of water resistivity; C – map of oil contamination for the pit area.

VES interpretation

The simplified geological model of the area consists of two horizontal layers: aquitard (above) and aquifer (below). Inside the first layer there are: artificial cover of sand and gravel in the east part of the area, products of drilling (mainly in the pit area) and contaminated zones (Table 1). Groundwater level is at the depth 1.5 -2 m inside the first layer (aquitard). That is why the contamination is situated above the groundwater level in aquitard.

Table 1

Values of resistivity and clay content for different soils of the cross-section and for contaminated zones

Part of section	Rho, Ω.m	Clay content, %
Upper part (aquitard) (0-4 m)	15 - 30	30 - 40
Artificial cover of sand and gravel	70 - 400	0 - 5
Drilling products	15 - 20	10 - 40
Lower part (aquifer)	50 - 100	0 - 10
Contaminated zones	< 12	> 50 (apparent value)

VES interpretation included qualitative analysis of all data and quantitative 2D VES interpretation. Typical VES curves were mainly of A and H types (Figure 3). High ρ_a values at small spacings are typical for a zone with sand and gravel cover. The deepest layer on VES curves with resistivity about 50 Ωm is the main aquifer. The low resistivity layer (15-30 Ωm) above is an aquitard. Contamination is clearly visible in the aquitard layer with the help of petrophysical modelling, which allows calculating resistivity of uncontaminated soils and estimating the difference between clean and contaminated soils.

VES data interpretation was performed with the Res2DInv software (Loke and Barker, 1995; 1996) using IPI2Win and X2IPI programs for VES data transformation (Bobachev, 1994, 2003) and Surfer (Golden software) for visualization.

The 2-D model created by the Res2DInv program consists of a number of rectangular blocks not exceeding the number of data points. The horizontal position and size of the blocks usually depend on the positions of data points. The depth of each row of blocks is approximately equal to corresponding depth of penetration for a given electrode spacing. Block thickness is the same in each row but the deeper row is 10% thicker than the previous row. The program is limited to 24 model layers, and in our case, the model had 7 layers. Using X2IPI program, we adopt a model with a block column below each sounding point; thus the number of blocks in each row is equal to the number of soundings. In this case we may create vertical sections, horizontal maps and arbitrary surface maps in the survey area using the coordinates of the blocks as a reference.

Examples of interpretation for profiles 5 and 9 are shown in Figure 4. A layer of minimum resistivity was found slightly above the groundwater level. We call this the "optimal layer", because it is the most favourable for a contamination study. Its existence at oil contaminated sites was confirmed by direct measurement, using Vertical Resistivity Probes (VRP) (Sauck, 1988). The low resistivity in this layer is due to intense bacterial action on residual hydrocarbons near the base of the vadose zone.

The optimal layer may be recognized in several profiles and may be used to prepare the resistivity map of the site for the depth 2 - 4 m (Figure 5). The dashed line shows the pit outline. From petrophysical modeling (see below), the boundary between contaminated and not contaminated soil is 12 Ωm. The 12 Ωm contour is shown as a heavier line. Two anomalies in the northern and the southern part of the pit show probable contaminated zones in agreement with geochemical data (Figure 3C).

Petrophysical modelling

Petrophysical modelling leads to a theoretical calculation of soil resistivity based on geological information about water and soil in the survey area. Soil resistivity depends on groundwater resistivity (as in Archie's formula (Archie, 1942); thus groundwater resistivity measurements are important for resistivity surveys.

The petrophysical approach used in this paper was developed by A. Ryjov in 1984 – 1990, and may be found in Ryjov (1987), Ryjov and Sudoplatov (1990) and Ryjov and Shevnin (2002).

Petrophysical model and forward problem modelling

There are many petrophysical models developed for the oil and gas industry (Archie, 1942; Waxman and Smits, 1968; Clavier *et al*., 1984; Johnson and Sen, 1988) and for near surface sediments (Rhoades *et al*., 1976; Ryjov, 1987; Ryjov and Sudoplatov, 1990; Tabbagh *et al*., 2002).

The conductivity of sandy and clayey soils was considered by Ryjov (1987) and Ryjov and Sudoplatov (1990),

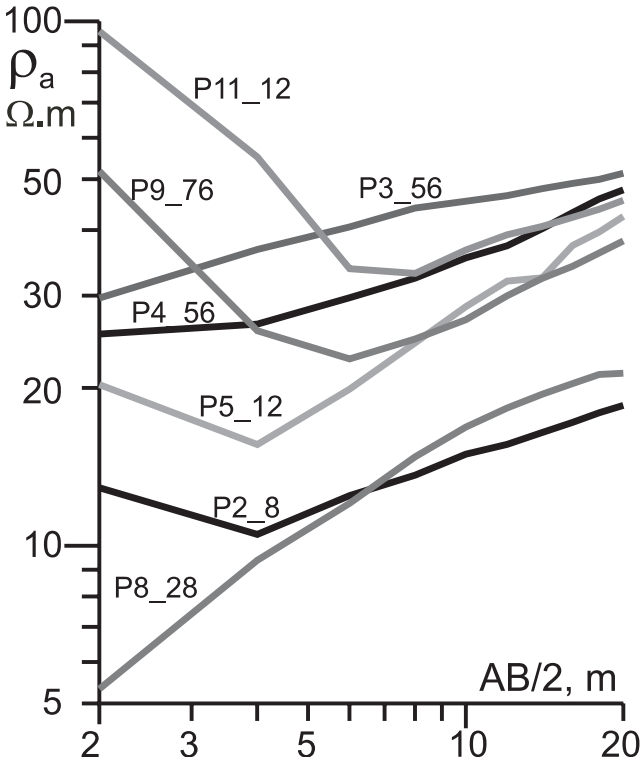

Fig. 3. First curve parameter indicates profile number, while second one the VES point.

taking into account the geometrical microstructure and electrochemical processes for a wide range of water salinity and clay content. The sand capillary radii are of 10^{-3}–10^{-4} m exceeding greatly the thickness of the electrical double layer (EDL). The EDL thickness depends on water salinity. At near surface conditions the fluid mineralization varies from 0.02 to 2 g/l and the EDL thickness ranges between 10^{-8} – 10^{-10} m. The pores of the clay component are assumed to be narrow because the average radii lie in the interval of 10^{-7} – 10^{-8} m and are comparable with the EDL thickness.

The walls of capillary ducts are non-conductive and depend on sand or clay electrochemical parameters, e.g. EDL and cation exchange capacity (CEC). Thus, the electrical properties of the sand-clay mixture are defined by the effective conductivities of wide or fine capillary systems.

Conductivities of sand (σ_{sand}) and clay (σ_{clay}) components may be described as follows:

$$\sigma_{sand} = \phi^{m}_{sand}\, \sigma_{sandcap} \tag{1}$$

$$\sigma_{clay} = \phi^{m}_{clay}\, \sigma_{claycap}\,, \tag{2}$$

where $\phi_{sand} = V_{sandpor} / V_{sand}$ and $\phi_{clay} = V_{claypor} / V_{clay}$ are the porosity values of sand and clay components; $V_{sandpor}$ and V_{sand} are the pore and sand total volume; $V_{claypor}$ and V_{clay} are the pore and total volume of the clay component; $\sigma_{sandcap}$ and $\sigma_{claycap}$ are the conductivity of a single capillary of sand and clay, *m* is the cementation exponent.

The average conductivity $\tilde{\sigma}_c$ of a capillary filled with water is a radially varying function σ(r) that depends on the electrical double layer properties:

$$\tilde{\sigma}_c = \frac{2}{r_c^2}\int_0^{r_c} r\sigma(r)dr\,, \tag{3}$$

where r_c is the capillary radius.

In the pore system of sand the average conductivity $\sigma_{sandcap}$ does not depend on the capillary radius and equals the free-water conductivity σ_w. The conductivity of free water relates strongly to salt type and salt concentration. The water solution conductivity can be approximated by a function of cation and anion concentrations considering the hydration effect (Ryjov, 1987):

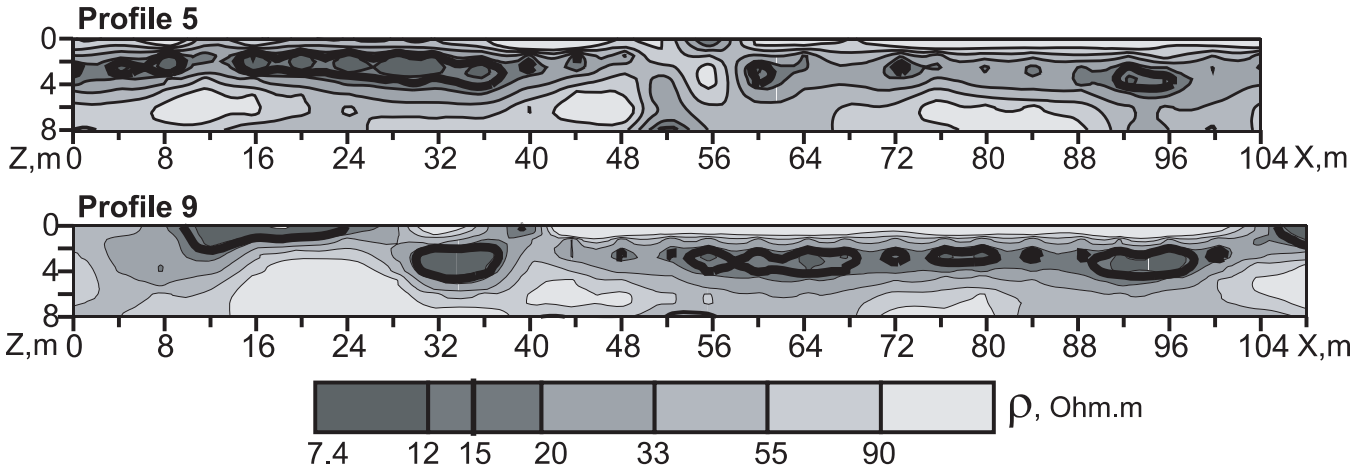

Fig. 4. Vertical resistivity cross-sections for profiles 5 and 9 after 2D interpretation with Res2DInv software.

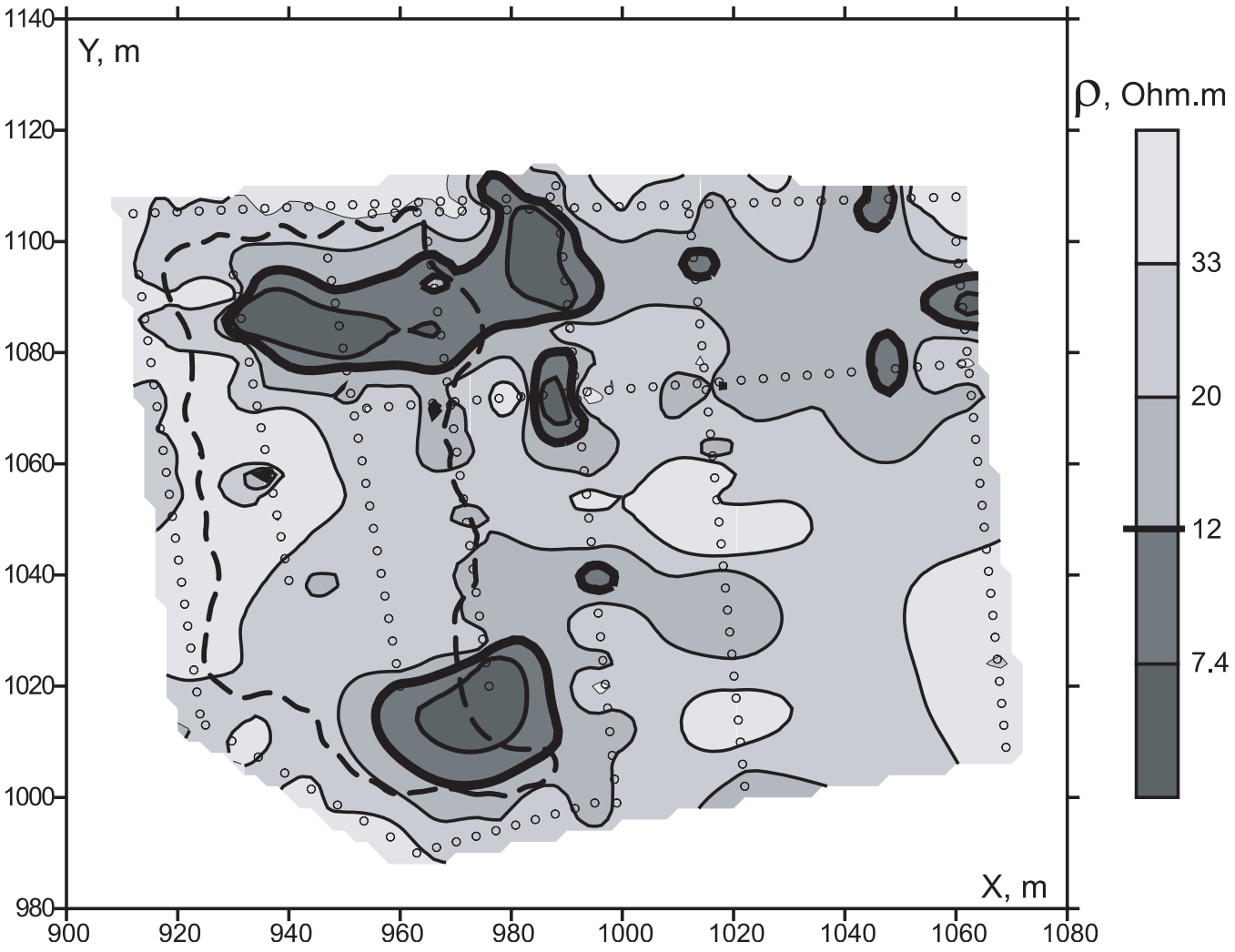

Fig. 5. Resistivity map for the optimal layer.

$$\sigma_w = \mathrm{F}\left\{z_c U_c C_c \exp\left(\frac{C_c}{1000zn}\right) + z_a U_a C_a \exp\left(\frac{C_a}{1000zn}\right)\right\}, \quad (4)$$

where z_c, z_a are the charges of ions or valence; F is the Faraday number, 96485 Q/mol; C_c and C_a are the cation and anion concentrations in the solution; U_c and U_a are the cation and anion mobilities and n is the hydration number.

This approach allows estimating the water conductivity for different salts such as NaCl, KCl, $Ca(HCO_3)_2$, $CaCl_2$, $MgCl_2$, $CaSO_4$, $NaHCO_3$, Na_2SO_4, etc., in a wide salinity range from 0.001 to 120 g/l at least.

For fine clay capillaries we use an analog to equation (4), where the concentration of the charges C is a function of the capillary radius C(r) and the clay cation exchange capacity (CEC): $C_i(r) = C_i^{DEL}(r) + C_i^{CEC}(r)$, where *i* is the index for cations or anions.

The concentration $C_i(x)$ of anions or cations with charge z_i in an electrical double layer is based on the Boltzmann equation (Fridrihsberg, 1984):

$$C_i(x) = C_{oi} \exp(-z_i F\psi(x)/RT), \quad (5)$$

where: C_{oi} is the cation or anion concentration in an electroneutral solution; x is the shortest distance from the given point in a liquid phase up to a solid phase; ψ(x) is the electric potential in a fluid at a current distance x from the capillary wall; R is the gas constant and T – absolute temperature in °K.

The microstructure of sandy – clayey soils may be described from the ideal packing concept for binary mixtures

of fine and coarse particles of quasi-spherical shapes (McGeary, 1961). When the clay concentration is less than the sand porosity, the clay particles fit inside the sand pores and do not modify the structure. When the clay concentration exceeds the sand porosity, the sand grains are embedded in the clay matrix.

The total porosity ϕ_t of sandy-clayey soils may be approximated by the following expressions (Ryjov and Sudoplatov, 1990; Marion *et al.,* 1992):

$$\phi = (\phi_{sand} - C_{clay}) + \phi_{clay}.C_{clay}, \quad C_{clay} < \phi_{sand} \qquad (6)$$

$$\phi = C_{clay}.\ \phi_{clay}, \quad C_{clay} \geq \phi_{sand}\ , \qquad (7)$$

where C_{clay} – is the volumetric clay content in a mixture.

When $C_{clay} > \phi_{sand}$ the conductivity σ_Σ corresponds to the effective conductivity σ_{clay} of the clay component. It depends on the conductivity of narrow channels, clay porosity and concentration.

$$\sigma_\Sigma = \sigma_{clay} C_{clay} \phi^m_{clay.} \qquad (8)$$

When $C_{clay} < \phi_{sand}$ the soil conductivity is defined by both the sand pore system and the fine clay capillaries.

A theoretical simulation of sandy-clayey mixture resistivity as a function of groundwater salinity shows an example of the template (Figure 6) for the following parameters: NaCl solution and full soil saturation, temperature 20°C, sand porosity 25%, clay porosity 55%, Cation Exchange Capacity (CEC) of clay 3 g/l. (Values from curves are clay content in % from 0 (sand) until 100 (clay)). The inclined dashed line is for water resistivity. If groundwater resistivity is 20 Ωm, we can estimate from Figure 6, water salinity (0.3 g/l) and lithological legend, where each type of soil (sand, sandy loam, loam, light (C3), medium (C2) and heavy (C1) clay) has its own resistivity interval.

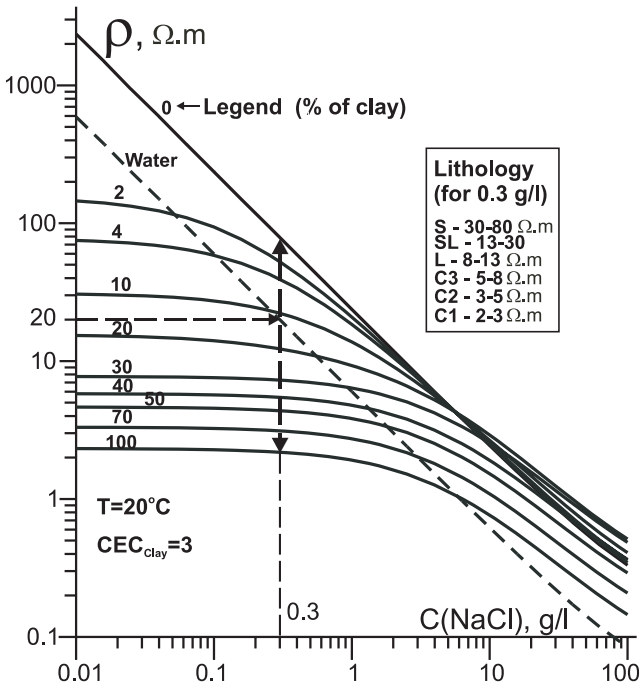

Fig. 6. Theoretical graphs of sandy-clayish soil resistivity from water salinity at CEC=3.

Interpretation of laboratory soil resistivity measurements as function of water salinity

If groundwater and soil resistivity at full saturation are known we may estimate from Figure 6 the soil lithology, the clay content and the porosity. This estimation was included in algorithm Petrofiz (Ryjov and Sudoplatov, 1990) from laboratory soil resistivity data ρ=f(C), where C is the water salinity. For this purpose we divide the soil sample into several subsamples, saturated by different NaCl solutions with salt concentration from 0.6 to 100 g/l. We measured the resistivity of each subsample using identical calibrated resistivimeters. Interpreting ρ(C) curve we are estimating clay content, soil porosity and cation exchange capacity. Some details of this technology may be found in Shevnin *et al*. (2004)

The ρ(C) graph for a soil sample obtained near monitoring well M-1 is presented in Figure 7, and its interpretation is in Table 2 together with two other samples obtained near sampling wells S-10 and S-2. The sample M-1 was taken in the reference area without contamination, whereas two other samples were taken in areas with strong and moderate contamination.

Table 2

Results of sample resistivity measurements' interpretation

Sampling site	Clay content %	Porosity %	CEC of clay, g/l	Fitting error, %
M-1	43	33	0.12	2.1
S-10	41	31	21	4.6
S-2	41	31	8	2.8

Note that clay content is close to 40% and the main difference between samples is in the CEC values. They are small for the clean reference site and large for the strongly contaminated site. These CEC estimates are apparent not a real values, but may be good indicators of mature petroleum contamination.

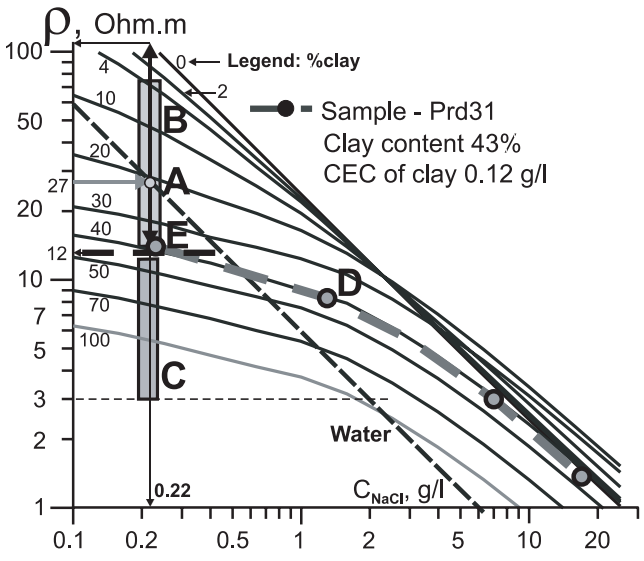

Fig. 7. Petrophysical analysis of water (A) and soil resistivity (D) together with VES data (B, C).

Petrophysical analysis of experimental information

The results of the petrophysical analysis are shown in Figure (7), based on a comparison of water and soil resistivity measurements, petrophysical modelling and VES resistivity statistical analysis. We intend to find a boundary resistivity value to distinguish between clean and contaminated soils. In Figure 7 is presented a theoretical template calculated for CEC value 0.12 g/l, estimated near the well M-1. A theoretical dependence of soil resistivity closer to the soil of the investigated site may be found from soil resistivity measurements for several different salinities (Figure 7). The theoretical palette of ρ=f(C) for different clay contents was calculated for a cation exchange capacity (CEC) of clay of 0.12 g/l. A groundwater resistivity value of 27 Ωm corresponds to the main aquifer. The salinity of this water (Figure 7, point A) is 0.22 g/1. The resistivity range between pure sand (Line 0) to sand with 40% of clay (Line 40) is from 14 to 100 Ωm. From statistical VES data analysis the resistivity of uncontaminated soil ranges from 12 to 70 Ωm. At water resistivity of 27 Ωm this yields a clay content of 4 to 40 % (Figure 7, grey rectangle B an line D). We consider soil resistivity values below 12 Ωm (line E) as indicating contaminated soil and accept this value as a boundary between clean and contaminated soils. Resistivity of contaminated soil is marked with rectangle C.

Recalculation of VES resistivity data into petrophysical parameters

Algorithm Petrofiz has been used for petrophysical modelling and soil resistivity data interpretation since 1984. Its applicability has been tested on many soils (Ryjov and Sudoplatov, 1990). In 2003 a new algorithm was developed for recalculation of soil resistivity from VES interpretation of petrophysical parameters. For petrophysical modelling about 15 soil parameters are used: water salinity, including types of anions and cations with their valence, hydration number, sorption constant and mobility; porosity, capillary radii, humidity, cementation exponent *m* and cation exchange capacity for sand and clay components, and temperature of soil. If we know soil resistivity from VES and water salinity from water resistivity measurements we may solve the inverse problem to estimate three soil parameters, e.g. clay content, porosity, and cation exchange capacity.

This algorithm allows recalculating vertical resistivity cross-sections and resistivity maps taking into account water salinity into sections and maps of petrophysical parameters.

The cross-section of profile 6 in Figure 8 can be divided visually into two parts: an upper one down to the depth 3-5 m and a lower one below depth 3-5 m. This division is clear and contrasting. Profile 6 is situated in the pit area and crosses two contaminated zones. In these zones all parameters have anomalous values.

The map in Figure 9A displays clay content for the optimal layer. From geological data the peak clay content in this area is 40%. With soil resistivity measurements and data interpretation we confirmed values close to 40%. But in Figure 9A there are zones with clay content up to 60%. These anomalous zones coincide with contaminated areas in the northern and southern parts of the pit. We successfully estimated the clay content in uncontaminated areas with the help of recalculation from resistivity data, but in the contaminated zones the clay content estimated from resistivity is not real and can be used only as a fairly good indicator of contamination. We assume that contamination can not change the clay content in a soil. But contamination does change the capillary properties and soil resistivity thus producing an apparent increase of clay content.

A similar situation is encountered with cation exchange capacity recalculated from resistivity (Figure 9B). CEC anomalies with values more than 23 g/l show the same zones in the pit as did clay content (Figure 9A) or petroleum contamination anomalies (Figure 2C).

Figure 10 presents three correlations between geological and geoelectrical parameters. (A) Correlation between hydrocarbon concentration and soil resistivity; (B) correlation between clay content from geological data and clay content estimated from resistivity; (C) correlation between cation exchange capacity estimated from soil samples and recalculated from resistivity data (1 = direct proportion and

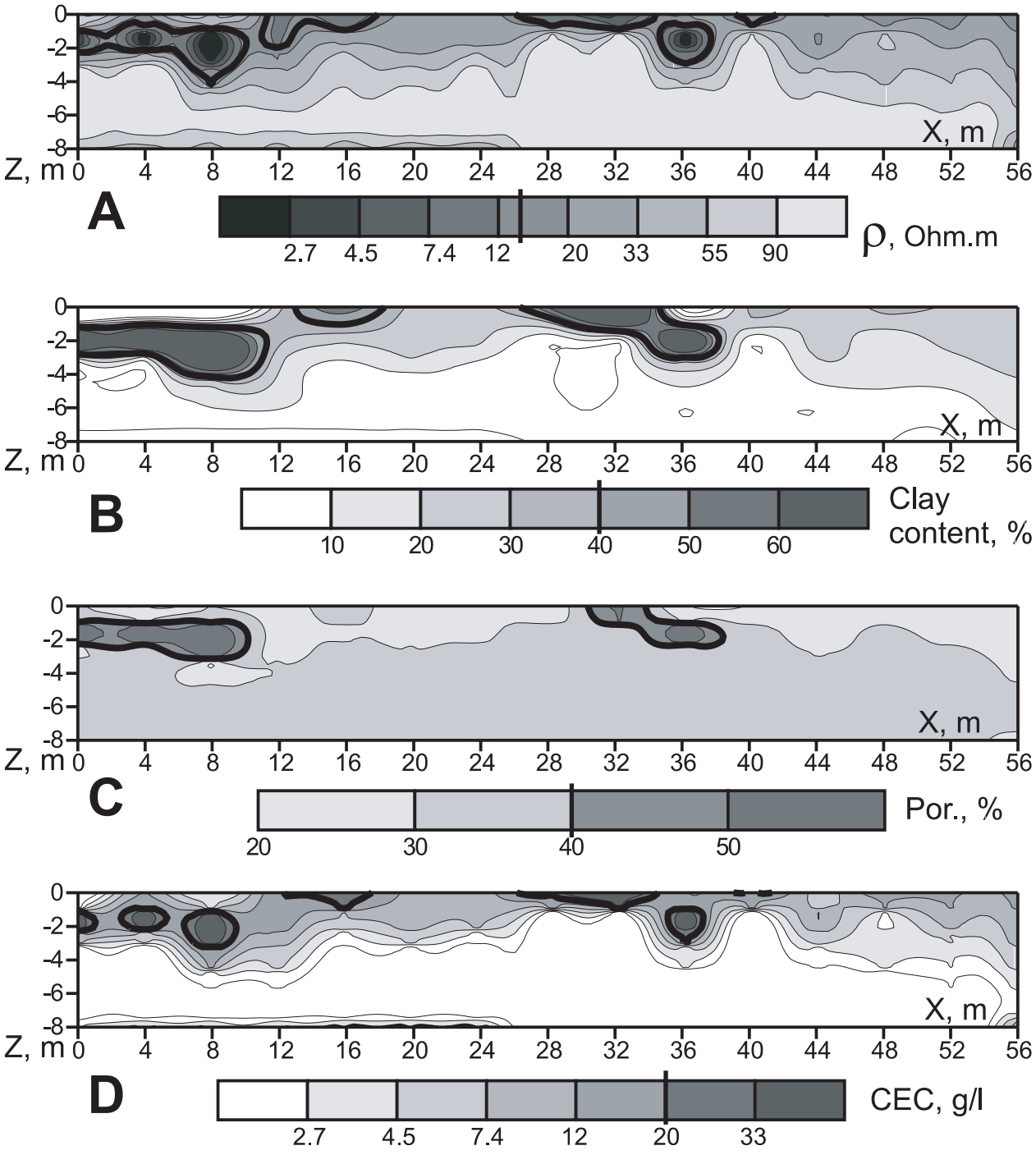

Fig. 8. Vertical cross-sections along profile 6 for the next parameters: A – resistivity; B – clay content; C – porosity; D – cation exchange capacity.

2 = practical approximation). The best correlation is shown between resistivity and contamination grade (A) that is the base for the resistivity method. Here the soil resistivity was measured on the same samples as for contamination. For graphs (B) and (C) the correlation is between direct estimation of clay content and CEC, and its integral estimation with the help of the resistivity method.

In Figure 11 the final results of the geoelectrical survey are presented. In the map there are different contours for resistivity, clay content, CEC and porosity. In the pit area there are three anomalous zones with crossings of four contours marked A, B, C. Outside of the pit only two parameters have crossed contours. Anomalies A and B coincide with geochemical anomalies, thus we consider these anomalies

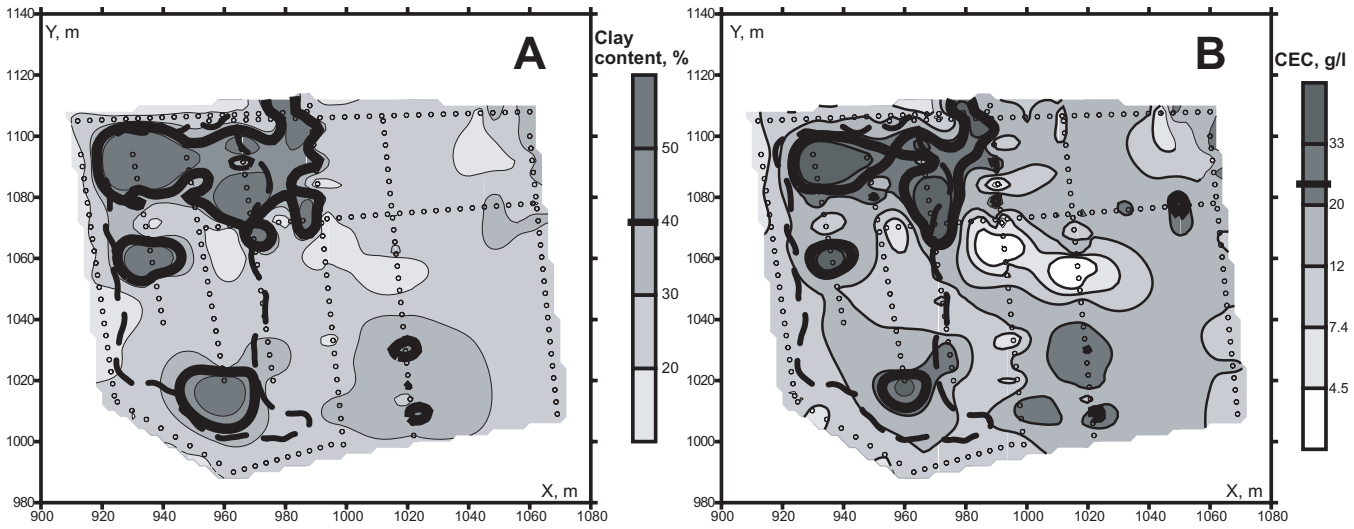

Fig. 9. Maps of clay content (A) and cation exchange capacity (B) recalculated from resistivity for the optimal layer.

as true contaminated zones. Anomaly C is located between sampling wells S -11 (13375 ppm) and S-12 (3566 ppm) in the zone of the geochemical gradient. But from geoelectrical data this anomaly looks like an oil contaminated zone. Also from geoelectrical data, an additional conductive zone D at X = 980, Y = 1110 was found outside the pit. This anomaly seems related to anomaly A, although its origin is not clear.

When integrating geochemical and geoelectrical information it is necessary to remember their differences. The geochemical method gives direct information about contamination, whereas the geoelectrical method gives indirect information. Geochemistry gives local data and geoelectric prospecting gives data integrated over a large volume. Productivity of the latter is nearly ten times greater than the former and the cost is 20 times lower. In this case a good integration of the two methods is very useful. Resistivity can be used first to outline contaminated zones, it can reduce the area for geochemical study to 20 - 40% of the total area. Results of a geoelectrical study are usually available in 3-5 days, whereas geochemical analysis in the laboratory may take as much as 2-3 weeks. A geoelectrical study does not affect the environment whereas drilling in contaminated zones can lead to aquifer contamination. It is important to obtain geoelectrical information before geochemical sampling to make this sampling more accurate in plan and depth.

CONCLUSIONS

1. A geoelectrical characterization of a contaminated site was carried out using vertical electrical sounding method as 2D Resistivity Imaging together with water and soil resistivity measurements. Contaminated areas were localized in plan and in depth, as low resistivity zones. The zones of maximum contamination were found in the pit area.

2. The correlation between soil resistivity and contamination shows that the VES method is effective in defining contaminated areas. The inverse correlation between geoelectrical parameters and concentration of contaminants confirms that oil-contamination in this site is “mature” and thus creates a low resistivity anomaly.

3. VES 2D interpretation was successful in finding an optimal layer in the lower part of the vadose zone. This layer is best for localizing contamination in plan.

4. Resistivity data can be recalculated into petrophysical parameters (clay content, porosity and cation exchange capacity). These parameters have standard values in uncontaminated zones and anomalous values in contaminated zones. They are useful for better differentiation of contaminated and uncontaminated zones. In contaminated zones the petrophysical parameters exhibit apparent anomalies caused by changes in soil capillaries.

ACKNOWLEDGMENTS

We are indebted to The Mexican Petroleum Institute, where this study was made. We acknowledge the valuable help of M. Sc. David Flores Hernández in the fieldwork. We sincerely thank Dr. A. Bobachev whose software was used in this study. We thank two reviewers for their comments that significantly improved the manuscript and Dr. Cinna Lomnitz the main editor of Geofísica Internacional for English corrections.

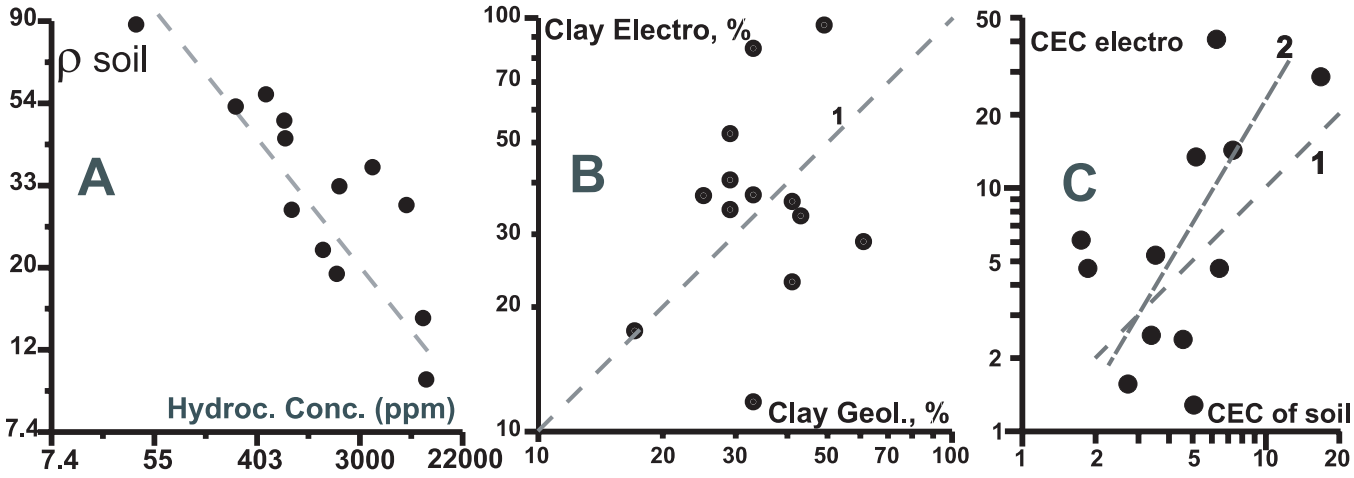

Fig. 10. Correlation graphs between geological and geoelectrical parameters.

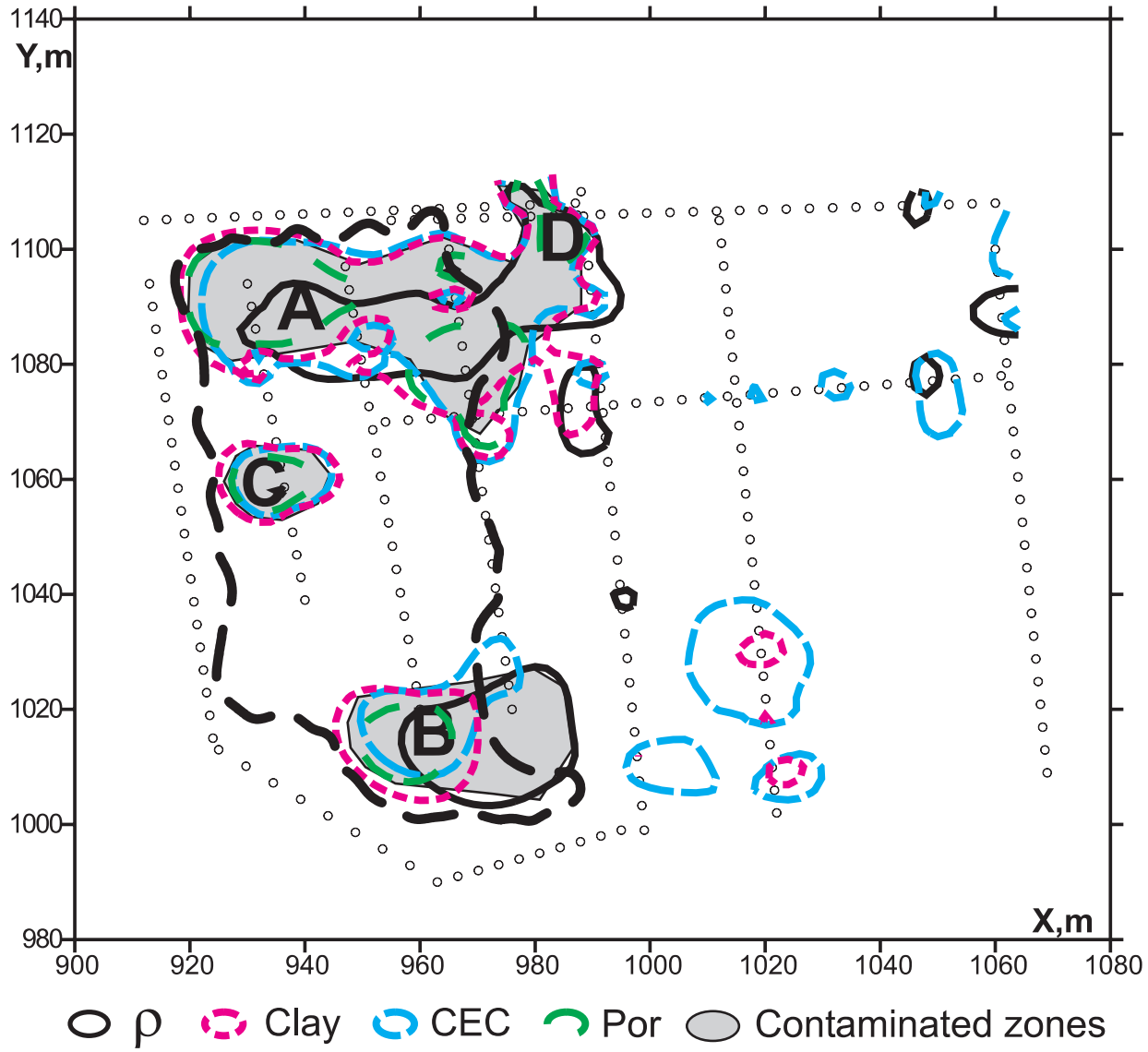

Fig. 11. Final result of geoelectrical survey, position of contaminated zones.

BIBLIOGRAPHY

ABDEL-AAL, G. Z., D. D. WERKEMA, W. A. SAUCK Jr. and E. ATEKWANA, 2001. Geophysical investigation of vadose zone conductivity anomalies at a former refinery site, Kalamazoo, ML. *In:* Proceedings of the Symposium on the Application of Geophysics to Engineering and Environmental Problems, 1-9.

ARCHIE, G. E., 1942. The Electric Resistivity Logs as an Aid in Determining some Reservoir Characteristics. SPE-AIME Transactions, 146, 54-62.

ATEKWANA, E., D. P. CASSIDY, C. MAGNUSON, A. L. ENDRES, D. D. WERKEMA, Jr. and W. A. SAUCK, 2001. Changes in geoelectrical properties accompanying microbial degradation of LNAPL. *In:* Proceedings of the Symposium on the Application of Geophysics to Engineering and Environmental Problems, 1-10.

BAILEY, N. J. L., H. R. KROUSE, C. R. EVANS and M. A. ROGERS, 1973. Alteration of Crude Oil by Waters and Bacteria - Evidence from Geochemical and Isotope Studies. *Amer. Ass. Petrol. Geol. Bull., 57,* 1276-1290.

BOBACHEV, A. A., 1994. IPI2Win software: http://geophys.geol.msu.ru/rec_labe.htm .

BOBACHEV, A.A., 2003, X2IPI software: http://geophys.geol.msu.ru/x2ipi/x2ipi.html .

BOUYOUCOS, G. J., 1962. Hydrometer method improved for making particle size analyses of soils. *Agron. J. 54(5)*, 464-465.

CLAVIER, C., G. COATES and J. DUMANOIR, 1984. Theoretical and Experimental Bases for the Dual-Water Model for Interpretation of Shaly Sands. *J. SPE,* 153-168.

FRIDRIHSBERG, D. A., 1984. Course of colloid chemistry. L.: Khimiya, -368 pp. (In Russian).

GRIFFITHS, D. H. and R. D. BARKER, 1993. Two-dimensional resistivity imaging and modelling in areas of complex geology. *J. Appl. Geophysics 29,* 211-226.

JOHNSON, D. L. and P. N. SEN, 1988. Dependence of the conductivity of a porous medium on electrolyte conductivity. *Physical Review B, 37, 7,* 3502-3510.

LOKE, M. H. and R. D. BARKER, 1995. Least-squares deconvolution of apparent resistivity pseudosectious. *Geophysics, 60,* 1682-1690.

LOKE, M. H. and R. D. BARKER, 1996. Rapid least-squares inversion of apparent resistivity pseudosections using a quasi-Newton method. *Geophysical Prospecting, 44,* 131-152.

MARION, D., A. NUR, H. YIN and D. HAN, 1992. Compressional velocity and porosity in sand-clay mixtures. *Geophysics, 57,* 554-563.

MCGEARY, R. K. 1961. Mechanical Packing of Spherical Particles. *J. Amer. Ceramic Soc., 44, 10,* 513-522.

MODIN, I. N., V. A. SHEVNIN, A. A. BOBATCHEV, D. K. BOLSHAKOV, D. A. LEONOV and M. L. VLADOV, 1997. Investigations of oil pollution with electrical prospecting methods. *In:* Proceedings of the 3rd EEGS-ES Meeting. Aarhus, Denmark, 267-270.

PEMEX, 2001. Annual Report. Petróleos Mexicanos. Mexico.

ROADES, J. D., P. A. C. RAATS and R. J. PRATHER, 1976. Effects of liquid-phase electrical conductivity, water content and surface conductivity on bulk soil electrical conductivity. *Soil Sci. Soc. Am. J., 40,* 651-655.

RYJOV, A. 1987. The main IP peculiarities of rocks // In the book “Application of IP method for mineral deposits' research”. Moscow, 1987, p. 5-23. (In Russian)

RYJOV, A. and V. SHEVNIN, 2002. Theoretical calculation of ground electrical resistivity and some examples of algorithm's application. *In:* Proceedings of the Symposium on the Application of Geophysics to Engineering and Environmental Problems. 10 pp.

RYJOV, A. A. and A. D. SUDOPLATOV, 1990. The calculation of specific electrical conductivity for sandy - clayed rocks and the usage of functional cross-plots for the decision of hydrogeological problems. *In:* “Scientific and technical achievements and advanced experience in the field of geology and mineral deposits research. Moscow, pp. 27-41. (In Russian).

SAUCK, W. A., 1998. A conceptual model for the geoelectrical response of LNAPL plumes in granular sediments. *In:* Proceedings of the Symposium on the Application of Geophysics to Engineering and Environmental Problems, pp. 805-817.

SAUCK, W. A., 2000. A model for the resistivity structure of LNAPL plumes and their environs in sandy sediments. *J. App. Geophys., 44,* 151 -165.

SHEVNIN, V., O. DELGADO RODRÍGUEZ, A. MOUSATOV and A. RYJOV, 2004. Soil resistivity measurements for clay content estimation and its application for petroleum contamination study. SAGEEP-2004, Colorado Springs. p. 396-408.

SHEVNIN, V., RYJOV, A., NAKAMURA, E., SÁNCHEZ, A., KOROLEV, V. and MOUSATOV, A., 2002. Study of oil pollution in Mexico with resistivity sounding. *In:* Proceedings of the Symposium on the Application of Geophysics to Engineering and Environmental Problems. 10 pp.

SHEVNIN, V., O. DELGADO-RODRÍGUEZ, A. MOUSATOV, E. NAKAMURA LABASTIDA and A. MEJÍA-AGUILAR, 2003. Oil pollution detection with resistivity sounding. *Geofís. Int., 2003. 42, 4,* 603-622.

TABBAGH, A., C. PANISSOD, R. GUÉRIN and P. COSENZA, 2002. Numerical modeling of the role of water and clay content in soils' and rocks' bulk electrical conductivity. *J. Geophys. Res., 107,* B11, 2318.

USEPA, 1983. Methods for Chemical Analysis of Water and Wastes. Environmental Protection Agency, Government Printing Office, Washington DC.

USEPA, 1995. Superfund program representative sampling guidance. Environmental Protection Agency, Soil, Vol. 1, EPA 540/R-95/141. Washington, DC.

USEPA, 2002. Exemption of Oil and Gas Exploration and Production Wastes from Federal Hazardous Waste Regulations. Environmental Protection Agency. EPA530-K-01-004. Washington, DC.

WAXMAN, M. H. and L. J. M. SMITS, 1968. Electrical conductivities in oil-bearing shaly sands. *J. Soc. Petrol. Eng., 8,* 107-122.

Vladimir Shevnin[1], Omar Delgado-Rodríguez[1], Luis Fernández-Linares[1], Héctor Zegarra Martínez[1], Aleksandr Mousatov[1] and Albert Ryjov[2]

[1] Mexican Petroleum Institute, Eje Central Lázaro Cárdenas 152, 07730 México, D.F., México
E-mail: vshevnin@imp.mx
[2] Moscow State Geological Prospecting Academy, Geophysical faculty, Volgina str., 9, 117485, Moscow, Russia.